Crossover from strong to weak confinement for excitons in shallow or narrow quantum wells

Rita Claudia Iotti and Lucio Claudio Andreani
Istituto Nazionale per la Fisica della Materia, Dipartimento di Fisica ''A. Volta,'' Università di Pavia, via Bassi 6, 27100 Pavia, Italy
(Received 18 November 1996; revised manuscript received 28 February 1997)

We present a theoretical study of the crossover from the two-dimensional (2D, separate confinement of the carriers) to the three-dimensional (3D, center-of-mass confinement) behavior of excitons in shallow or narrow quantum wells (QW's). Exciton binding energies and oscillator strengths are calculated by diagonalizing the Hamiltonian on a large nonorthogonal basis set. We prove that the oscillator strength per unit area has a minimum at the crossover, in analogy with the similar phenomenon occurring for the QW to thin-film crossover on increasing the well thickness, and in agreement with the analytic results of a simplified δ-potential model. Numerical results are obtained for GaAs/Al_x Ga_{1-x}As and In_xGa_{1-x}As/GaAs systems. Our approach can also be applied to obtain an accurate description of excitons in QW's with arbitrary values of the offsets (positive or negative) and also for very narrow wells. In particular, the crossover from 2D to 3D behavior in narrow GaAs/Al_xGa_{1-x}As QW's is investigated: the maximum binding energy of the direct exciton in GaAs/AlAs QW's is found to be $\sim$26 meV and to occur between one and two monolayers. [S0163-1829(97)03431-0]

I. INTRODUCTION

Excitons in quantum wells[1–3] (QW's) are known to be characterized by two regimes. For a well thickness $L \sim a_B$, where a_B is the effective Bohr radius, the exciton binding energy is smaller than the confinement energy of the carriers and electrons and holes are separately confined: this is the strong confinement [or quasi-two-dimensional (2D)] regime, in which the exciton binding energy and the oscillator strength per unit area increase on reducing the thickness because of compression of the electron-hole wave function in the layer planes. On the other hand for $L \gg a_B$ the binding energy is larger than the carrier quantization energy: this is the so-called weak confinement [or three-dimensional (3D)] regime, in which the center-of-mass motion of the exciton is quantized as a whole, and the oscillator strength per unit area is proportional to the film thickness. Thus the oscillator strength per unit area must have a minimum at the crossover from strong to weak confinement. The minimum occurs[4] at $L \sim 2.5a_B$, as was experimentally observed in CdTe/(Cd,Zn)Te QW's.[5] The regimes of strong and weak confinement occur also in systems of lower dimensionality, e.g., for excitons in quantum wires[6] and microcrystals or quantum dots[7–9] (although the size-dependent oscillator strength has a different behavior in zero-dimensional systems[10]).

If the confining potentials are taken as infinite the exciton becomes two-dimensional when the well width goes to zero:[11] however the fact that band discontinuities are finite in real structures gives rise to interesting and nontrivial behavior for narrow wells. Starting from the strong confinement regime and decreasing the thickness, the binding energy and the oscillator strength go through a maximum and decrease when the carrier wave functions leak into the barriers:[12] for vanishing thickness, the exciton becomes that of the barrier material. For ultranarrow/shallow QW's (i.e., when the well width and/or the band offsets are very small so that the carrier wave functions are mostly in the barrier region) it becomes more appropriate to think of the carriers and excitons of the ''barrier'' material as the unperturbed states, while the attractive potential of the ''well'' region acts as an impurity layer and produces localization of these states. Instead of a confinement energy, the relevant quantity is now a localization energy, which is measured from the barrier band edge (Fig. 1). As long as the localization energies of the carriers are larger than the exciton binding energy, there is separate confinement of electron and hole levels and the exciton is still in the strong confinement regime (although the single-particle levels may largely extend in the barrier material). On the other hand, if the localization energy of the carriers is smaller than the exciton binding energy, the barrier exciton can be in a situation where its center of mass is localized as a whole: this is a weak confinement regime, in the sense that there is no separate localization of electron and hole levels within the exciton wave function. In this limit the localization length of the excitonic center of mass increases on decreasing the thickness, producing an increase of the oscillator strength per unit area. Thus the behavior of QW excitons on decreasing the thickness is the mirror image of the behavior for thick wells: starting from the strong confinement regime, there is a crossover to weak confinement, and the oscillator

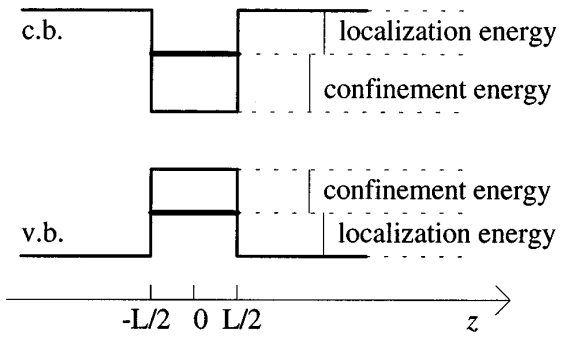

FIG. 1. Schematic representation of conduction- and valence-band profiles, showing localization and confinement energies for electron and hole levels in relation to the band offsets.

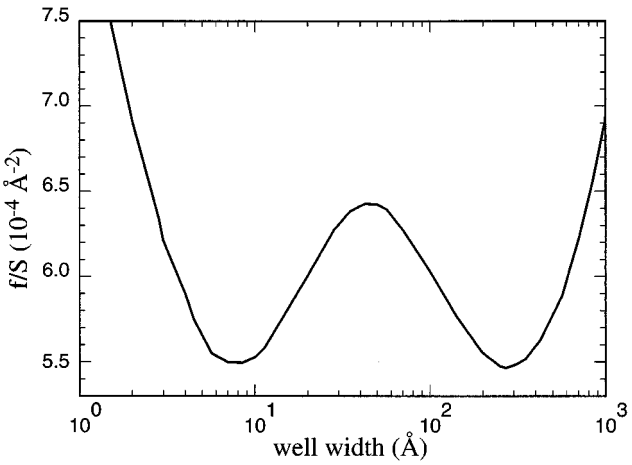

FIG. 2. Oscillator strength per unit surface of the lowest heavy-hole exciton transition, as a function of the well thickness, for a $GaAs/Al_{0.15}Ga_{0.85}As$ QW. Parameters employed in the calculation: see Table I and text.

strength per unit area must have a minimum. This weak confinement regime can occur in shallow QW's (i.e., when the barrier height is very small) or in ultranarrow QW's.

The above-described behavior of the oscillator strength per unit area is illustrated in Fig. 2, which refers to the ground state heavy-hole exciton in $GaAs/Al_{0.15}Ga_{0.85}As$ QW's. The curve is calculated by the model described later in this paper. The first minimum of the oscillator strength occurs at a thickness of about 8 Å, while the second minimum is found around 300 Å.

The phenomena described above have an analog in the behavior of excitons bound to impurities in bulk semiconductors.[13,14] It is well known that excitons weakly bound to impurity centers have a very large oscillator strength, which allows the contribution of bound excitons to be seen in absorption even if the impurity concentration is small. This phenomenon is usually referred to as the ''giant oscillator strength:[13]'' it takes place when the exciton is in the weak confinement regime, i.e., when its center of mass is localized and coupling of the center of mass to the relative motion induced by the impurity potential is weak. When this condition is satisfied the oscillator strength depends on the localization energy $E_{\rm loc}$ like $f \propto E_{\rm loc}^{-3/2}$ for the three-dimensional impurity case[13] (see also Sec. II A below).

The purpose of this work is to investigate the crossover from 2D (strong confinement) to 3D (weak confinement) behavior in shallow or narrow QW's by means of an envelope-function model. The main issues are (i) to develop an accurate yet flexible method, which can be applied to the whole range of thicknesses and for any values of the band offsets; (ii) to study the minimum of the oscillator strength in GaAs/(Al,Ga)As and (In,Ga)As/GaAs structures; (iii) to calculate the maximum value of the binding energy and to describe the crossover to the barrier exciton, taking into account the variation of the band parameters and of the dielectric constant.

The number of existing theoretical studies of excitons in QW's is large. Most authors have concentrated on the strong confinement regime.[11,12,15–21] The thin-film regime and the QW to thin-film crossover were investigated in a few papers.[22,23,4,24] A few studies of the weak confinement regime in shallow[25,26] or narrow[27–29] QW's have recently appeared. The present work is also related to the studies of monolayer and submonolayer insertions, like InAs in GaAs.[30,31] A more detailed comparison with existing literature is given in the course of the paper.

In Sec. II we first present a simplified model for the crossover from strong to weak confinement, then describe the full model and illustrate the method of solution. In Sec. III we present several results for the minimum of the oscillator strength in GaAs/(Al,Ga)As and (In,Ga)As/GaAs systems. In Sec. IV we apply the more accurate theory (including also conduction-band nonparabolicity and the dielectric mismatch) to a study of the maximum value of the exciton binding energy and of the crossover to the barrier exciton in GaAs/(Al,Ga)As QW's. Section V contains concluding remarks.

II. MODEL AND METHOD

A. Simplified model

In order to get a qualitative picture of the physics involved in the crossover from strong to weak confinement we have approximated the shallow or narrow QW by δ-like potentials.[32] This is a reasonable choice if the exciton radius is much larger than the well thickness and the exciton wave function is mostly in the barrier region. This model allows us to obtain a few simple results for the behavior of the oscillator strength in terms of the variational parameters, and yields physical insight which usefully complements the more accurate numerical calculations described in the next subsection. The exciton Hamiltonian in this simplified model is

$$H = E_g^b - \frac{\hbar^2 \nabla_e^2}{2m_e^*} - \frac{\hbar^2 \nabla_h^2}{2m_h^*} - V_e L\,\delta(z_e) - V_h L\,\delta(z_h) - \frac{e^2}{\epsilon |\mathbf{r}_e - \mathbf{r}_h|}, \tag{1}$$

where E_g^b is the band gap of the barrier material. The quantities $V_e L$ and $V_h L$ have the dimensions of energy times length: one can think of V_e, V_h as being the conduction- and valence-band offsets, while L is the well thickness. To study the model Hamiltonian (1) we have employed two one-parameter variational wave functions suitable to describe the two limiting regimes of 2D and 3D excitons. The variational wave function for the strong confinement regime is

$$F_s(\rho, z_e, z_h) = N e^{-\alpha\rho} e^{-|z_e|/l_e} e^{-|z_h|/l_h}, \tag{2}$$

where ρ is the in-plane relative coordinate, $l_{e,h} = \hbar^2/(m_{e,h} V_{e,h} L)$ are the localization lengths of electron and hole in the δ-like potentials, and α is a variational parameter which represents the inverse of the electron-hole separation. N is a normalization constant. The wave function (2) is analogous to the separable wave function for excitons in QW's of medium thickness.[11] The variational wave function for the weak confinement regime is

$$F_w(\rho, z, Z) = \widetilde{N} e^{-r/a_B} e^{-|Z|/l_c}, \tag{3}$$

where $z(Z)$ is the relative (center-of-mass) coordinate along the growth direction, $r=\sqrt{\rho^2+z^2}$, a_B is the bulk Bohr radius, and l_c is a variational parameter which represents the localization length of the excitonic center of mass. $\widetilde{N}$ is again a normalization constant.

In the particular case $m_e^*=m_h^*=m^*$ and $V_e=V_h=V$ some interesting observations can be made. The localization energy of the carriers is $m^*(VL)^2/(2\hbar^2)$. The condition of weak confinement (i.e., that this localization energy is much smaller than the bulk effective Rydberg $\mathcal{R}$) is equivalent to $VL \ll \mathcal{R}a_B$. In this limit the value of the variational parameter l_c that minimizes the total energy is given by

$$l_c=\frac{\hbar^2}{(2m^*)(2V)L} \tag{4}$$

and is equal to the confinement length of a particle of mass $M=2m^*$ in a δ-like attractive potential $2VL$. The exciton transition energy for $VL \ll \mathcal{R}a_B$ is given to lowest order in L by

$$E_{\rm ex} \simeq E_g^b - \mathcal{R} - \frac{4m^*L^2V^2}{\hbar^2}. \tag{5}$$

Defining the localization energy of the barrier exciton by $E_{\rm ex}=E_g^b-\mathcal{R}-E_{\rm loc}$, we see that the localization energy in this limit is $E_{\rm loc} \simeq 4m^*L^2V^2/\hbar^2$. The barrier exciton energy for $L \to 0$ is correctly recovered [the separable wave function (2) fails to reproduce this limiting value and produces $E_{\rm ex}=E_g^b$].

In the strong confinement regime ($VL \gg \mathcal{R}a_B$) the value of α that minimizes the total energy is

$$\alpha=\frac{2}{a_B}\left(1-\frac{4\mathcal{R}a_B}{VL}\right). \tag{6}$$

The exciton binding energy in the limit $VL/\mathcal{R}a_B \to \infty$ reaches the two-dimensional value $4\mathcal{R}$.

It is then possible to produce a crossover from strong to weak confinement by varying the ratio $VL/\mathcal{R}a_B$. For a fixed structure, this crossover can be obtained by varying the well width L. The curves of the excitonic transition energies as a function of the well width obtained for both the wave functions (2) and (3) cross at a certain thickness L_0:[32] the strong confinement wave function (2) yields the lowest energy for $L>L_0$, while the weak confinement wave function (3) gives the lowest energy for $L<L_0$.

In the case of strong confinement ($L>L_0$), the oscillator strength per unit surface can be evaluated for the separable wave function (2) as a function of the variational parameter α:

$$\frac{f_{\hat{\epsilon}}}{S}=g\frac{2}{m_0\hbar\omega}|\langle u_v|\hat{\boldsymbol{\epsilon}}\cdot\mathbf{p}|u_c\rangle|^2\left|\int F_{\rm s}(\rho=0,z,z)\,dz\right|^2$$
$$=g\frac{2}{m_0\hbar\omega}|\langle u_v|\hat{\boldsymbol{\epsilon}}\cdot\mathbf{p}|u_c\rangle|^2\frac{2\alpha^2}{\pi}\frac{4l_el_h}{(l_e+l_h)^2}, \tag{7}$$

where g is the spin-orbit factor,[3] $\hat{\boldsymbol{\epsilon}}$ is the polarization vector, and u_v, u_c are the Bloch functions of the valence and conduction bands at the Γ point. The oscillator strength per unit area in the strong confinement regime decreases with decreasing well thickness, due to the decrease of the inverse electron-hole separation α [Eq. (6)]. We emphasize that this behavior corresponds to that of QW's when electron and hole states are mostly found in the barrier regions.

With a wave function of the form (3) the oscillator strength per unit surface is given as

$$\frac{f_{\hat{\epsilon}}}{S}=g\frac{2}{m_0\hbar\omega}|\langle u_v|\hat{\boldsymbol{\epsilon}}\cdot\mathbf{p}|u_c\rangle|^2\left|\int F_w(\rho=0,z=0,Z)\,dZ\right|^2$$
$$=g\frac{2}{m_0\hbar\omega}|\langle u_v|\hat{\boldsymbol{\epsilon}}\cdot\mathbf{p}|u_c\rangle|^2\frac{1}{\pi a_B^3}4l_c. \tag{8}$$

Thus in the weak confinement regime the oscillator strength per unit surface increases on reducing the well thickness due to the increase of the localization length l_c for the center-of-mass motion [Eq. (4)]. Using also Eq. (5) we see that the oscillator strength per unit area depends on the localization energy as $f/S \propto E_{\rm loc}^{-1/2}$. This trend has to be compared with the ''giant oscillator strength'' of excitons weakly bound to impurity states,[13] as discussed in the Introduction, which yields $f/S \propto E_{\rm loc}^{-3/2}$.

The behavior found in the two limiting regimes proves that a minimum of the oscillator strength per unit area must occur at the crossover from strong to weak confinement. A numerical treatment shows that the trend $f/S \propto E_{\rm loc}^{-1/2}$ characteristic of the weak confinement regime occurs for thicknesses L smaller than about one tenth of the crossover value. These results are useful for comparing with those of the model presented below.

B. Accurate model

In the framework of the effective-mass approximation,[1,33,34] a more realistic Hamiltonian can be written as

$$H=E_g-\frac{\hbar^2}{2\mu(z_e,z_h)}\left\{\frac{1}{\rho}\left[\frac{\partial}{\partial\rho}\left(\rho\frac{\partial}{\partial\rho}\right)\right]\right\}-\frac{\hbar^2}{2}\frac{\partial}{\partial z_e}\frac{1}{m_e^*(z_e)}\frac{\partial}{\partial z_e}$$
$$-\frac{\hbar^2}{2}\frac{\partial}{\partial z_h}\frac{1}{m_h^*(z_h)}\frac{\partial}{\partial z_h}+V_e\Theta\left(z_e^2-\frac{L^2}{4}\right)$$
$$+V_h\Theta\left(z_h^2-\frac{L^2}{4}\right)-\frac{e^2}{\epsilon\sqrt{\rho^2+(z_e-z_h)^2}}+V_{\rm im}(\rho,z_e,z_h)$$
$$+V_{\rm self}(z_e)+V_{\rm self}(z_h), \tag{9}$$

where we have defined the in-plane relative ($\vec{\rho}$,$\mathbf{k}$) and center-of-mass ($\mathbf{R}$,$\mathbf{K}$) coordinates in the following way:

$$\mathbf{K}=\mathbf{k}_e+\mathbf{k}_h \quad \mathbf{R}=\frac{1}{2}(\vec{\rho}_e+\vec{\rho}_h), \tag{10}$$

$$\mathbf{k}=\frac{1}{2}(\mathbf{k}_e-\mathbf{k}_h) \quad \vec{\rho}=\vec{\rho}_e-\vec{\rho}_h, \tag{11}$$

and dropped the center-of-mass terms, being interested in the case of optically created excitons. E_g is now the band gap of the well material. The z axis is chosen along the growth direction: z_e and z_h indicate the electron and hole positions along z. m_e^* is the conduction-band effective mass. The hole

dynamics is described by the Luttinger Hamiltonian in diagonal approximation. Within this picture the hole effective mass along the z direction, m_h^*, and the exciton reduced mass in the x-y plane, μ, are related to the Luttinger parameters by the following relations for [001]-grown QW's:[33,35]

$$\frac{1}{m_{h,l}^*}=\frac{1}{m_0}(\gamma_1\mp 2\gamma_2), \tag{12}$$

$$\frac{1}{\mu_{h,l}}=\frac{1}{m_e^*}+\frac{1}{m_0}(\gamma_1\pm\gamma_2), \tag{13}$$

where m_0 is the free-electron mass and the subscript h (l) and the upper (lower) signs refer to the heavy- (light-) hole exciton. All effective masses are z dependent, since they assume different values in well and barrier materials. V_e and V_h are the conduction- and valence-band offsets, and $\Theta[z^2-(L^2/4)]$ is the Heaviside function. ϵ is the background dielectric constant of the well material, $V_{\rm im}$ represents the corrections to the Coulomb potential due to the dielectric constant mismatch between well and barrier and $V_{\rm self}(z_e)$, $V_{\rm self}(z_h)$ are the corresponding single-particle self-energies.[16]

To solve the excitonic problem we proceed through a variational calculation consisting of diagonalizing the Hamiltonian (9) on an appropriate basis. The form of the basis functions has to be flexible enough in order to give a unified description of both regimes of strong and weak confinement. As the envelope function of optically active exciton states is even with respect to the inversion $(z_e,z_h)\rightarrow(-z_e,-z_h)$, we expand it in the following nonorthogonal set:

$$F(\rho,z_e,z_h)=\sum_k^{2n} c_k\phi_k(\rho,z_e,z_h),\quad k=(k_1,k_2,k_3), \tag{14}$$

$$\phi_k=N_k\exp(-\alpha_{k_1}\rho)\exp\left(-\frac{1}{2}\beta_{k_2}z_e^2\right)\exp\left(-\frac{1}{2}\beta_{k_3}z_h^2\right),\quad k=1,\ldots,n, \tag{15}$$

$$\phi_k=N_k z_e z_h\exp(-\alpha_{k_1}\rho)\exp\left(-\frac{1}{2}\beta_{k_2}z_e^2\right)\exp\left(-\frac{1}{2}\beta_{k_3}z_h^2\right),\quad k=n+1,\ldots,2n, \tag{16}$$

where α_{k_1}, β_{k_2}, and β_{k_3} are fixed parameters, chosen to cover a broad physical range. An expansion of the exciton wave function upon a basis very similar to set (15) [but neglecting states (16)] has already been proposed.[29]

Exciton eigenenergies and wave functions are then determined by minimizing the expectation value of the Hamiltonian (9) with respect to the variational coefficients c_k, i.e., by solving a generalized eigenvalue problem of the form

$$\sum_{k=1}^{2n} c_k(H_{k,l}-S_{k,l}E)=0,\quad \forall l, \tag{17}$$

where $H_{k,l}$ and $S_{k,l}$ are the Hamiltonian and the overlap matrix elements

$$H_{k,l}=\langle\phi_k|H|\phi_l\rangle,\quad S_{k,l}=\langle\phi_k|\phi_l\rangle. \tag{18}$$

The binding energy E_b of the excitonic ground state is defined as the difference between the lowest transition energies evaluated without and with the Coulomb coupling between electron and hole:

$$E_b=E_g+E_h+E_e-E_{\rm ex}, \tag{19}$$

where E_h and E_e are the ground state energies of the hole and electron confined in the QW (including dielectric self-energies), and $E_{\rm ex}$ is the lowest transition energy of the Hamiltonian (9). Once the values of the variational coefficients that minimize the total energy have been determined, it is possible to evaluate the oscillator strength of the transition between the fundamental state of the crystal and the exciton ground state:

$$\frac{f_{\hat\epsilon}}{S}=g\frac{2}{m_0E_{\rm ex}}|\langle u_v|\hat\epsilon\cdot\mathbf{p}|u_c\rangle|^2\left|\sum_{k=1}^{2n} c_k\int_{-\infty}^{+\infty}\phi_k(\rho=0,z,z)dz\right|^2. \tag{20}$$

The expansion in a large basis set (15), (16) is equivalent to keeping all discrete and continuum levels in an expansion over subbands; therefore the exciton does not have to be associated to a given pair of subbands. The use of a Gaussian basis set allows us to evaluate analytically most matrix elements (except for the Coulomb potential one) in terms of the error functions. The evaluation of the Coulombic matrix element is described in the Appendix. Our model allows us to include the dielectric constant mismatch between well and barrier materials. In particular, the use of a Gaussian basis set combined with the procedure described in the Appendix makes it possible to sum the contributions of the infinite image charges:[36,18] this is clearly necessary in order to reproduce the barrier exciton with the proper dielectric constant as $L\rightarrow 0$.

The effective-mass mismatch between the constituent materials and the current conserving boundary conditions[37,34] are automatically taken into account in Eq. (9) by writing the kinetic terms in a symmetrized form.[38] For an accurate evaluation of the exciton binding energy and oscillator strength, corrections due to the conduction-band nonparabolicity have been estimated by the Rössler formulas[39] for bulk band nonparabolicities, assuming an energy-dependent electron effective mass.[18] Bulk nonparabolicity is taken into account in both well and barrier materials. For thick structures only the parameters of the well (including nonparabolicity) play a role, since the exciton is largely confined; on the other hand, in the limit $L\rightarrow 0$ only the barrier parameters become of significance. More details are given in the Appendix. Valence-band mixing effects are neglected in our model, due to the fact that we describe the hole dynamics by the Luttinger Hamiltonian in diagonal approximation.

III. CROSSOVER FROM STRONG TO WEAK CONFINEMENT AND MINIMUM OF OSCILLATOR STRENGTH

In order to study the crossover from strong to weak confinement, we have applied the model and method described in Sec. II B to different structures. As the excitonic oscillator

TABLE I. Material parameters of binary compounds employed in the calculations. Most values are taken from Ref. 40.

Parameter	GaAs	AlAs	InAs
m_e^*	0.0665	0.15	0.0225
γ_1	6.85	3.45	19.67
γ_2	2.10	0.68	8.37
ε	12.53	10.06	14.6
E_p (eV)	25.7	25.7	18.24
E_g (eV)	1.5192	3.1132	0.4105

strength is not very sensitive to the effects of conduction-band nonparabolicity and of dielectric mismatch, and since the minimum of the oscillator strength is easier to observe in shallow QW's where the material parameters differ only slightly, we have performed calculations assuming parabolic conduction bands and taking the barrier dielectric constant equal to the well one. We focus on the ground state heavy-hole exciton. Parameters employed are summarized in Table I for binary compounds. For what concerns ternary alloys, dielectric constant and conduction- and valence-band effective masses have been obtained by linear interpolation between the values of Table I. For $Al_xGa_{1-x}As$ with $x \leqslant 0.4$ the energy gap has been calculated by the Casey-Panish formula $\Delta E_g(x) = 1.247x$ eV, assuming the valence-band offset to be 35% of the total band gap discontinuity. For $In_xGa_{1-x}As$ the valence band offset is taken to be 40% of the total band gap discontinuity, defined as the difference between the band gap of GaAs and the heavy-hole gap $E_g^{\rm str}(x)$ of biaxially strained $In_xGa_{1-x}As$;[41] the quantity $E_p = 2|\langle u_c|\mathbf{p}|u_v\rangle|^2/m_0$ has been approximated by $E_g^{\rm str}(x)/m_e^*(x)$, where m_e^* is the conduction-band effective mass of the alloy.

A. GaAs/$Al_xGa_{1-x}As$ system

We have already shown in Fig. 2 the oscillator strength per unit area in GaAs/$Al_{0.15}Ga_{0.85}As$ QW's in a wide range of thicknesses. Figure 2 illustrates the behavior discussed in the Introduction, namely, the minima of the oscillator strength occurring at the crossover from strong to weak confinement in both very thick and very thin wells. The quasi-two-dimensional (strong confinement) regime of the exciton occurs between the two minima, i.e., from about 8 to 300 Å. Figure 2 also shows that the present basis gives a good representation of the exciton wave function in the whole range of thicknesses.

In Fig. 3 we plot the results obtained for GaAs/$Al_xGa_{1-x}As$ QW's for different aluminum concentrations. For the lowest concentration ($x = 0.01$) the minimum of the oscillator strength per unit surface occurs at $L \sim 100$ Å: this agrees with the value for the crossover from strong to weak confinement obtained from measurements on the exciton in a magnetic field.[26] On increasing the Al concentration the position of the minimum is rapidly displaced towards narrower wells, due to the increase of the localization energy. This produces the crossing of the curves corresponding to different values of x, showing that the oscillator strength per unit area is not always an increasing function of concentration. The behavior of the oscillator strength shown in Fig. 3 could

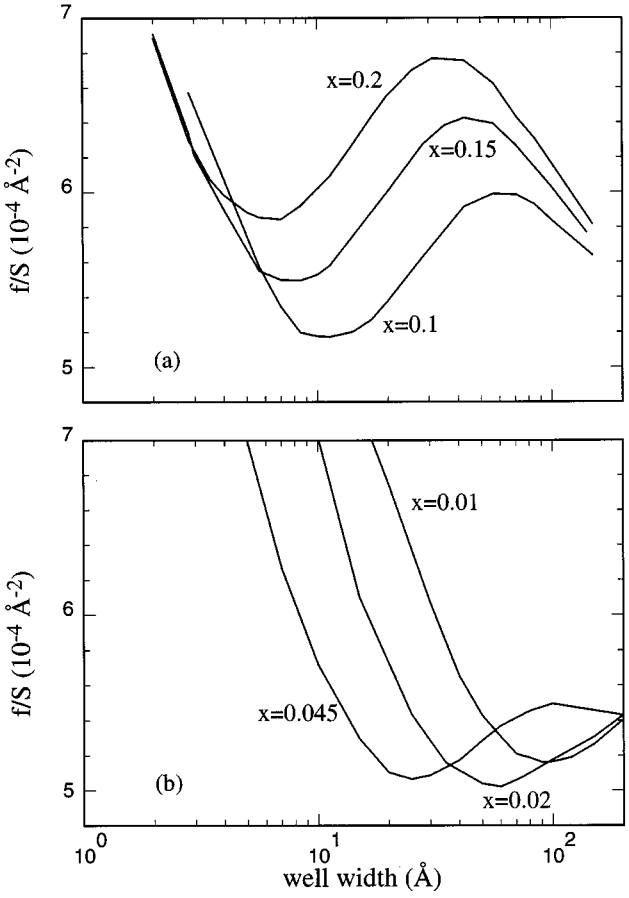

FIG. 3. Calculated heavy-hole exciton oscillator strengths per unit surface for several GaAs/$Al_xGa_{1-x}As$ QW's of different thicknesses and aluminum concentrations. The figure has been divided in two parts for clarity. Parameters employed in the calculation: see Table I and text.

be probed, e.g., by absorption, reflectance, or modulated reflectance spectroscopy on high-quality samples.

To have a deeper insight in the mechanism of the crossover, we have looked also at other quantities characterizing excitons in QW's. We define in-plane and along-z radii $\langle\rho\rangle, \langle z\rangle$ by

$$\langle\rho\rangle^2 = \left\langle \psi_{\rm exc}\left|\frac{\rho^2}{2}\right|\psi_{\rm exc}\right\rangle, \quad \langle z\rangle^2 = \langle\psi_{\rm exc}|(z_e - z_h)^2|\psi_{\rm exc}\rangle \tag{21}$$

(the definitions are such that both $\langle\rho\rangle, \langle z\rangle$ tend to the same value in the 3D limit). In Fig. 4 we plot the binding energy, the in-plane and along-z radii, and the probability of electron and hole confinement in the well region for a GaAs/$Al_{0.15}Ga_{0.85}As$ QW, as a function of the well thickness. The comparison of Fig. 4(a) with Fig. 2 shows, first of all, that the maximum of the oscillator strength per unit area occurs when the binding energy assumes its maximum value, i.e., when the exciton is mostly 2D and is in the strong-confinement regime.[12] On the contrary, there is no peculiar feature in the binding energy plot at the thicknesses L_1 and L_2 (with $L_1 < L_2$) corresponding to the two minima of f/S. Figure 4(b) shows that when $L \leqslant L_1$ or $L \geqslant L_2$ the exciton tends to recover a spherical shape, i.e., a 3D character, as it

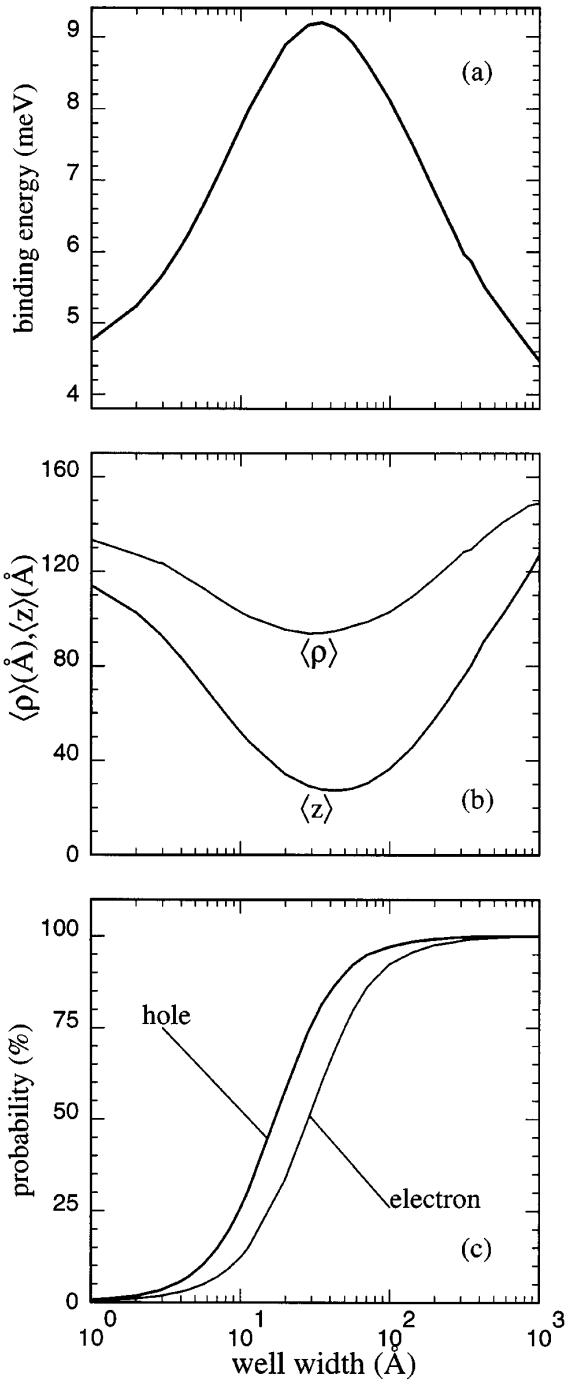

FIG. 4. (a) Binding energy, (b) in-plane and along-z exciton radii [see Eq. (21)] and (c) probability of electron and hole localization in the well region for a $GaAs/Al_{0.15}Ga_{0.85}As$ QW, as a function of the well thickness. Parameters as in Fig. 2.

can be expected from the fact that the exciton in the weak confinement regime is essentially bulklike. Figure 4(c) eventually shows that the crossover to weak confinement for $L \sim L_1$ corresponds to $\sim 10\%$ probability of finding the carriers in the well region. This demonstrates that the exciton can be in strong confinement regime even if the electron and hole states are partly delocalized, and that the weak confinement regime cannot be simply associated to wave function leakage in the barriers. In conclusion the comparison of Fig. 4 with Fig. 2 shows that the clearest signature of the crossover from strong to weak confinement is provided by the minimum of the oscillator strength per unit area, while neither the binding energy nor the confinement probability allow us to characterize the crossover.

TABLE II. Binding energies (in meV) of the ground state hh1-cb1 exciton in shallow $GaAs/Al_xGa_{1-x}As$ QW's of different aluminum concentration ($L = 200$ Å). Column two: experimental binding energy from $1s$-$2s$ splitting. Column three: absolute determination of binding energy. Column four: previous theoretical values. Column five: present work.

x	$E_{(1s-2s)}+E_{b,2s}$ [a]	E_b(abs.) [a]	E_b(theor.) [a]	E_b(theor.) [b]
0.01	5.9 ± 0.1	6.0 ± 0.5	5.4	5.6
0.02	6.4 ± 0.1	6.4 ± 0.5	5.7	6.1
0.045	7.0 ± 0.1	6.5 ± 0.5	6.1	6.4

[a]Reference 42.
[b]This work.

The results of Figs. 2 and 4(a) may be compared to those of simplified models. For large widths beyond the second minimum the exciton is in regime of center-of-mass confinement and the ground state is expected to be close to that of a particle of mass $M^* = m_e^* + m_h^*$ quantized in a box of thickness $L - 2d$ (where d is a dead-layer thickness).[4] Defining the quantization energy through $E_{ex} = E_g - \mathcal{R}^* + E_q$, we have verified that the binding energies reported in Fig. 4(a) correspond to the expected behavior $E_q \simeq \pi^2\hbar^2/[2M(L - 2d)^2]$, with a dead-layer thickness slightly larger than the exciton radius. Also, the oscillator strength per unit area in Fig. 2 increases $\propto L$, as expected. For a well width L below the first minimum one might try to verify the trends found for the simplified model of Sec. II A, namely, that the oscillator strength increases like $f \propto L^{-1}$ and the localization energy decreases like $E_{loc} \propto L^2$ on decreasing thickness, leading to $f \propto E_{loc}^{-1/2}$. Actually this behavior is established only for well widths smaller than about one tenth of the crossover value: for such very small well widths the complete calculation converges slowly with respect to the number of basis functions, so that the dependencies characteristic of the weak coupling regime could not be verified. A different choice of the basis functions (e.g., which are separable in center of mass and relative coordinates) could perform better in the extreme weak confinement regime: the basis set (15) and (16), on the other hand, allows a good description of the exciton states in a very wide range of well widths, as shown, e.g., by the results of Figs. 2 and 4.

To test the validity of our model, we have calculated the exciton binding energy for various Al concentrations and compared with available experimental data.[42] The results are shown in Table II for $x = 0.01$, 0.02, and 0.045. Calculated values are in good agreement with experimental results and an increase of the binding energy with respect to previous theoretical values is found.

B. $In_xGa_{1-x}As/GaAs$ system

Calculated oscillator strengths per unit area for $In_xGa_{1-x}As/GaAs$ QW's are plotted in Fig. 5, as a function of the well width and for $x = 0.05$, 0.1, and 0.17. Within our model which neglects valence-band mixing, the presence of

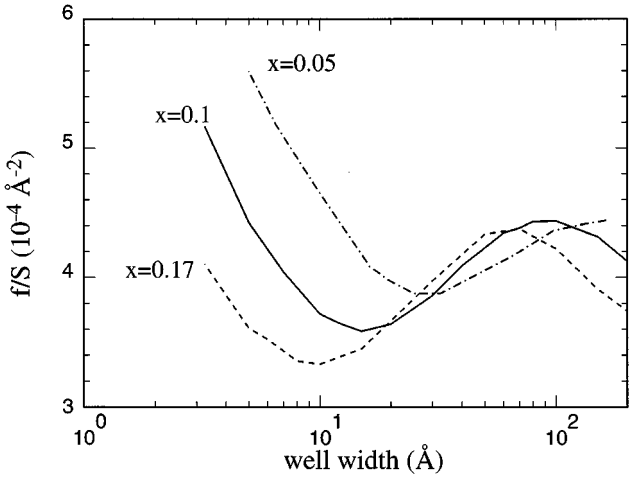

FIG. 5. Oscillator strength per unit surface of the lowest heavy-hole exciton transition, as a function of the well thickness, for $In_xGa_{1-x}As/GaAs$ strained QW's with different indium concentrations.

strain due to pseudomorphic growth enters only via the values of the band offsets. The crossing of the curves for $L \sim 100$ Å is due to the competing effects of quantum confinement, which increases with the In concentration, and of the reduction of the effective mass for the $In_xGa_{1-x}As$ alloy: for larger thicknesses the wave function is well confined for all ternary compositions and the oscillator strength decreases with concentration due to the reduction of the effective mass, while for widths below the maximum confinement increases strongly with concentration and produces an increase of the oscillator strength. For even smaller widths the exciton goes over to the weak confinement regime and the oscillator strength per unit surface has a minimum: like for shallow GaAs/(Al,Ga)As QW's, the minimum lies in a range of thicknesses accessible to experimental verification by optical spectroscopies.

A comparison with available experimental results for the oscillator strength[43] is presented in Fig. 6 for the cases of $x=0.1$ and $x=0.17$. The dotted lines refer, for comparison, to the results of a variational calculation assuming the hole to be completely confined in the well region.[38] The agreement between calculated and measured values is quite satisfactory and shows that a proper account of delocalization of both carriers is quite important for an accurate evaluation of the oscillator strengths. The thicknesses of the samples used in the experiments are unfortunately too large to be in the region of the minimum.

C. Monolayer and submonolayer insertions

Recent experimental evidence has pointed out the surprisingly high excitonic oscillator strength for monolayer insertions of InAs in GaAs.[30,31] Moreover, the excitonic oscillator strength is found to be higher than expected and not much dependent on concentration for submonolayers of InAs in GaAs,[28] i.e., when coverage of the impurity plane is only partial. When trying to apply an effective-mass theory to these situations caution is of course needed: nevertheless, we believe that our results allow us to make a few useful considerations.

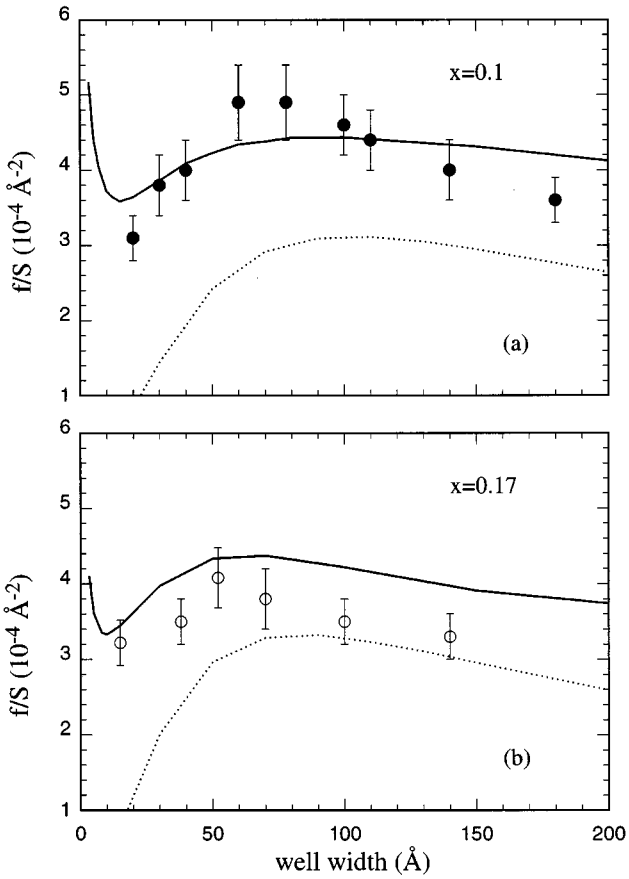

FIG. 6. Calculated heavy-hole exciton oscillator strengths per unit surface in strained $In_xGa_{1-x}As/GaAs$ QW's with $x=0.1$ and $x=0.17$. Full lines: present approach. Dotted lines: variational calculation assuming the hole to be completely confined in the well region (Ref. 38). Circles/disks: experimental points (Ref. 43).

Although the single-particle energy levels for one monolayer of InAs in GaAs cannot be calculated by an effective-mass theory, tight binding[30,44] as well as pseudopotential[45] calculations show that electron and hole levels bound to the attractive potential provided by the impurity plane do exist. These levels are of course very extended in the ''barrier'' material. The first question is now whether the exciton bound to the monolayer is in strong or weak confinement, i.e., whether independently localized single-particle levels exist or rather it is the center of mass of the exciton which is localized as a whole. The results of the present model, obtained with the thickness corresponding to one monolayer (about 2.83 Å for InAs in GaAs), indicate that the first situation is realized, i.e., independent localization of electrons and holes takes place. We believe that this prediction of the effective-mass calculation can be trusted: in fact, a similar conclusion was reached by a one-dimensional tight-binding model for the exciton (see the first of Ref. 30). If we tentatively calculate the oscillator strength per unit area of one monolayer InAs in GaAs, we find a value of 3.1×10^{-4} $Å^{-2}$, which is in good agreement with the experimental result (3.0×10^{-4} $Å^{-2}$).[30] While it cannot be excluded that this perfect agreement is to some extent fortuitous, it appears that the effective-mass theory gives a fair representation of the excitonic wave function: this may be related to the fact

that the localization length of the carrier is large and therefore the carriers' envelope function is slowly varying.

The problem of submonolayer insertions, which is raising considerable interest in the past few years,[27,28] is even more complex since in-plane islands are likely to be formed during the growth. When the coverage is decreased below a certain limit, the situation is likely to resemble more and more the exciton weakly bound to impurity centers,[13] where the localization length increases in all directions on reducing confinement. However it should also be remarked that absorption measurements for light propagating close to the growth direction are performed with a beam area which is much wider than the island size and spacing, so that what is measured is the surface average of the oscillator strength of all excitons falling within the laser spot: thus on reducing the coverage the effects of decreasing island number and of increasing exciton localization length are likely to compensate, at least partially. Therefore it can still be expected that a minimum of the oscillator strength per unit area occurs in submonolayers of InAs in GaAs on reducing the coverage, and that the oscillator strength per unit surface can attain values comparable to those for much thicker wells. Both of these conclusions appear to be in agreement with the experimental results reported in Ref. 28, although a quantitative comparison with experiment would of course not be warranted.

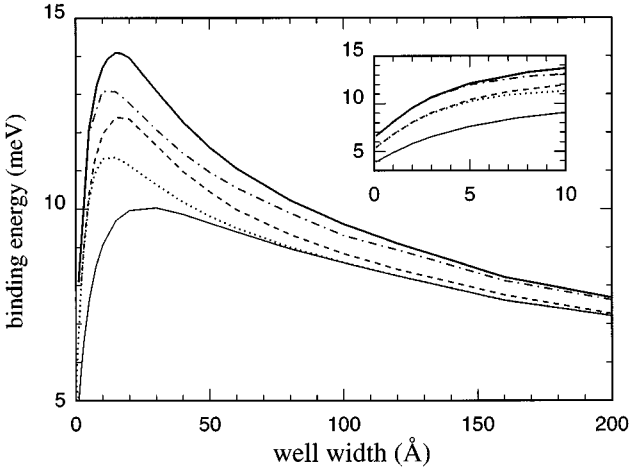

FIG. 7. Binding energy of the ground state heavy-hole exciton in a GaAs/$Al_{0.4}Ga_{0.6}$As QW as a function of the well thickness. Calculations have been performed on different assumptions. Thin solid line: assuming equal effective masses and dielectric constants for well and barrier materials and a parabolic conduction band. Dotted line: including the effective-mass mismatch. Dashed line: including the effective-mass mismatch and the conduction-band nonparabolicity. Dashed-dotted line: including the effective-mass mismatch and the difference of dielectric constants, but with a parabolic conduction band. Thick solid line: full calculation, including all effects mentioned above and also the self-energy corrections.

IV. ACCURATE RESULTS FOR DEEP GaAs/Al_xGa_{1-x}As QUANTUM WELLS

The present approach can also be applied to deep QW's and it allows us to include in the theory the effects of conduction-band nonparabolicity and of the dielectric constant mismatch. These effects are essential in order to give an accurate evaluation of the binding energy when the well becomes very narrow and the exciton becomes that of the barrier. Moreover, the binding energy in the quasi-two-dimensional regime may be strongly increased by the effects of conduction-band nonparabolicity and of the dielectric mismatch:[15,16,18,19] it was shown in Ref. 18 that these effects lead to a binding energy in GaAs/Al_xGa_{1-x}As structures which can become higher than the 2D limit of four times the bulk Rydberg. This prediction was later confirmed experimentally.[46] However the basis set used in Ref. 18 was such that calculations were restricted to well widths larger than 30 Å, where the binding energy is still increasing with reducing thickness. The present method now allows us to calculate the binding energy for any well thickness, and therefore to investigate the maximum value of the binding energy in narrow GaAs/Al_xGa_{1-x}As structures.

In Fig. 7 we present the calculated binding energy of the ground state heavy-hole exciton in a GaAs/$Al_{0.4}Ga_{0.6}$As QW as a function of the well thickness. Calculations have been performed under different assumptions, and therefore at different levels of accuracy. The corrections due to the effective-mass mismatch, the dielectric constant discontinuity, and the conduction-band nonparabolicity lead to an increase of the binding energy with respect to the calculation performed assuming the same material parameters for the well and barrier regions. The effective-mass mismatch contributes to the enhancement of the binding energy only for narrow wells, i.e., when the carrier leakage into the barriers is significant. The effect of the difference in dielectric constants persists up to a greater thickness due to the long range nature of the polarization effects. Although the behavior shown in Fig. 7 is of course qualitatively similar to the well-known results of Greene and Bajaj,[12] the inclusion of the various effects leads to quantitative differences: in particular, the maximum value of the binding energy is larger and it occurs at smaller thicknesses compared to the results obtained with the same material parameters. In the inset of Fig. 7 we show how the binding energy tends to the barrier value (5.96 meV with the parameters of Table I, compared to 3.61 meV for GaAs) for very narrow wells. The neglect of valence-band mixing is responsible for the small difference between these bulk binding energies and the values in the spherical approximation.[35]

In Fig. 8 we present the results of the full calculation of the heavy-hole exciton binding energy for three concentrations: the results of Fig. 8 therefore correspond to the full line in Fig. 7 and include difference in band parameters, conduction-band nonparabolicity, and dielectric mismatch. It should be noticed that the lowest exciton state in GaAs/AlAs QW's with $L \leqslant 36$ Å is the indirect Γ-X exciton: what is plotted in Fig. 8 is the binding energy of the direct exciton, which is not the lowest one, but can still be detected with excitation spectroscopy. It can be seen from Fig. 8 that for the case of GaAs/AlAs QW's a maximum value much greater than the 2D limiting value of the well material ($\sim$ 16 meV) is found, due to the combined effects of quantum confinement and variation of material parameters. The maximum value of the binding energy is about 26 meV and is reached at a thickness between one and two monolayers.

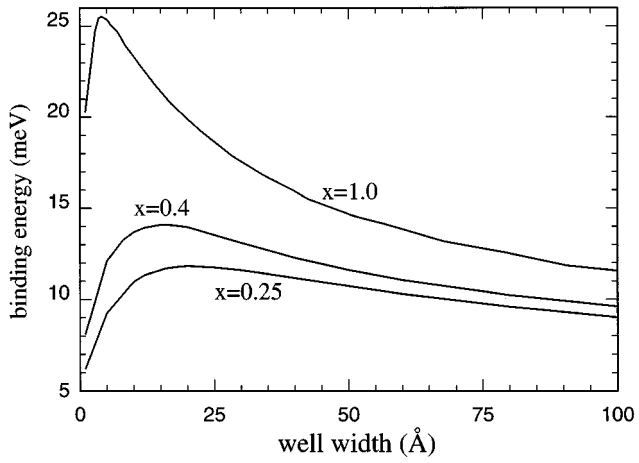

FIG. 8. Accurate results for the binding energy of the ground state heavy-hole exciton in GaAs/$Al_xGa_{1-x}As$ QW's, as a function of the well thickness, for different aluminum concentrations.

V. CONCLUSIONS

We have presented a method to study, within an envelope-function model, the crossover from strong to weak confinement occurring for excitons in shallow or narrow QW's, i.e., QW's in which either the band offsets or the well thickness are small. Our approach is based on the diagonalization of the exciton Hamiltonian on a finite basis set, which allows us to represent the exciton wave function in a wide range of thicknesses.

We have demonstrated that the oscillator strength per unit surface has a minimum at the crossover, in analogy with what happens at the QW to thin-film crossover on increasing thickness. The application of our approach to (In,Ga)As/GaAs and GaAs/(Al,Ga)As shallow QW's has shown that the minimum occurs at thicknesses accessible to experimental verification by optical spectroscopy. It has been argued that the exciton bound to monolayer insertions like InAs in GaAs is still in the strong confinement regime, but can go over to weak confinement when coverage of the impurity plane is only partial, thereby accounting for the high excitonic oscillator strength observed in submonolayer insertions.

The method can also be applied to QW's with arbitrary values of the offsets (positive or negative) and allows an accurate evaluation of the exciton binding energy, taking into account the effect of conduction-band nonparabolicity and the variation of band parameters and dielectric constant between well and barrier materials. The maximum value of the binding energy of the direct heavy-hole exciton in GaAs/AlAs QW's is found to be about 26 meV and to occur at a thickness between one and two monolayers.

Note added. Recent cathodoluminescence measurements[47] on a sample containing GaAs/$Al_{0.35}Ga_{0.65}As$ QW's of thicknesses from one to eight monolayers give evidence for the predicted minimum of the oscillator strength. The qualitative behavior of the signal intensity agrees with that shown in Fig. 3, and the minimum of the intensity occurs at a thickness of three monolayers.

ACKNOWLEDGMENTS

We are most grateful to M. Di Ventra and G. C. La Rocca for useful conversations and suggestions. We are also much indebted to A. Bitz and R. Schwabe for sending us their unpublished cathodoluminescence results.

APPENDIX: COULOMBIC MATRIX ELEMENTS AND CONDUCTION-BAND NONPARABOLICITY

In the case of equal dielectric constants between the two materials, the Coulombic matrix element $H_{k,l}^{\mathrm{Coul}}$ between basis functions (15), (16) can be written as

$$H_{k,l}^{\mathrm{Coul}}=-\frac{2\pi}{\epsilon}N_kN_l\int_0^\infty \rho\,d\rho\int_{-\infty}^{+\infty}dz_e\int_{-\infty}^{+\infty}dz_h f(z_e,z_h)\times\frac{1}{\sqrt{\rho^2+(z_e-z_h)^2}}e^{-(\alpha_{k_1}+\alpha_{l_1})\rho}e^{-1/2(\beta_{k_2}+\beta_{l_2})z_e^2}\times e^{-1/2(\beta_{k_3}+\beta_{l_3})z_h^2},\tag{A1}$$

where

$$f(z_e,z_h)=\begin{cases}1 & \text{if } 1\leqslant k,l\leqslant n\\ z_ez_h & \text{if } 1\leqslant k\leqslant n \text{ and } n+1\leqslant l\leqslant 2n\\ & \text{or vice versa}\\ z_e^2z_h^2 & \text{if } n+1\leqslant k,l\leqslant 2n.\end{cases}$$

Expression (A1) cannot be analytically evaluated, so we proceed as follows. First, we performed a numerical calculation, employing a one-dimensional Gauss quadrature method, of the ρ integral. The result depends only on $\alpha|z_e-z_h|$, where $\alpha=\alpha_{k_1}+\alpha_{l_1}$: we fitted this quantity with a linear combination of Gaussian functions in $\alpha|z_e-z_h|$,

$$\int_0^\infty d\rho\frac{\rho}{\sqrt{\rho^2+(z_e-z_h)^2}}e^{-\alpha\rho}\cong\frac{1}{\alpha}f(\alpha|z_e-z_h|)\cong\frac{1}{\alpha}\sum_k f_ke^{-\eta_k(\alpha|z_e-z_h|)^2}.\tag{A2}$$

The fit was performed by fixing the quantities η_k and determining the coefficients f_k through a least-square method. The original matrix element can now be expressed as an integral in z_e, z_h,

$$H_{k,l}^{\mathrm{Coul}}\cong-\frac{2\pi}{\epsilon}N_kN_l\frac{1}{\alpha}\sum_k f_k\int_{-\infty}^{+\infty}dz_e\int_{-\infty}^{+\infty}dz_h f(z_e,z_h)\times\exp\left[-\eta_k(\alpha|z_e-z_h|)^2-\frac{1}{2}(\beta_{k_2}+\beta_{l_2})z_e^2-\frac{1}{2}(\beta_{k_3}+\beta_{l_3})z_h^2\right],\tag{A3}$$

which can be analytically solved.

In order to include in the theory the effects of the dielectric mismatch, the presence of polarization charges at the interfaces can be taken into account with the image-charges method.[16] Several cases have to be considered, corresponding to all possible positions of electron and hole in the different layers. The resulting expressions are lengthy and are not reported here. Some of the integrals are treated by the

fitting procedure described above, while the remaining ones are evaluated by expressing the Coulomb potential through a two-dimensional Fourier integral,[17] evaluating the z_e, z_h integrals in terms of the error function, and computing the remaining integral in Fourier space by Gaussian quadrature. We stress that the structure of the basis allows us to sum the contributions of the infinite image charges, and thereby to take into account the difference in dielectric constants without any approximations (besides numerical ones).

To reproduce the correct excitonic behavior in the case of narrow wells and high confinement energies, we have estimated the corrections due to conduction-band nonparabolicity assuming an energy-dependent electron effective mass and using the Rössler formulas[39] for bulk band nonparabolicities. This leads to a nonparabolicity effect on the in-plane effective mass which is about three times larger than the effect on the longitudinal effective mass (see Ref. 18 for more details). For very thin wells the confinement energy becomes so large that the approximate formulas of Ref. 39 are not valid anymore; however in this limit the well parameters are irrelevant and only the barrier parameters matter. For the sake of simplicity, in the case of very thin wells the energy-dependent electron effective mass of the well material has been extrapolated to the Γ-point value of the barrier material. Different interpolation schemes could be conceived which, however, would not change the results. Similarly, for very thick wells the electron effective mass of the barrier is extrapolated to the Γ-point value of the well material.

[1] G. Bastard, *Wave Mechanics Applied to Semiconductor Heterostrucures* (Les éditions de physique, Paris, 1992).

[2] See, e.g., *Optics of Excitons in Confined Systems*, Proceedings of the Fourth International Meeting, edited by F. Bassani, G. C. La Rocca, and A. Quattropani [Nuovo Cimento D **17**, 1211 (1995)], and previous conference proceedings referenced therein.

[3] L. C. Andreani, in *Confined Electrons and Photons: New Physics and Devices*, edited by E. Burstein and C. Weisbuch (Plenum Press, New York, 1995), p. 57.

[4] L. C. Andreani, A. D'Andrea, and R. Del Sole, Phys. Lett. A **168**, 451 (1992).

[5] Y. Merle d'Aubigné, H. Mariette, N. Magnea, H. Tuffigo, R. T. Cox, G. Lentz, Le si Dang, J.-L. Pautrat, and A. Wasiela, J. Cryst. Growth **101**, 650 (1990).

[6] R. Cingolani and R. Rinaldi, Riv. Nuovo Cimento **16**, 9 (1993).

[7] Al. L. Efros and A. L. Efros, Fiz. Tekh. Poluprovodn. **16**, 1209 (1982) [Sov. Phys. Semicond. **16**, 772 (1982)]; L. E. Brus, J. Chem. Phys. **80**, 4403 (1984).

[8] L. Bányai and S. W. Koch, *Semiconductor Quantum Dots* (World Scientific, Singapore, 1993).

[9] For a recent review, see papers J. Lumin. **70**, 1 (1996).

[10] T. Takagahara, Phys. Rev. B **36**, 9293 (1987).

[11] G. Bastard, E. E. Mendez, L. L. Chang, and L. Esaki, Phys. Rev. B **26**, 1974 (1982).

[12] R. Greene and K. K. Bajaj, Solid State Commun. **45**, 831 (1983); R. Greene, K. K. Bajaj, and D. E. Phelps, Phys. Rev. B **29**, 1807 (1984).

[13] E. I. Rashba and G. E. Gurgenishvili, Fiz. Tverd. Tela **4**, 1029 (1962) [Sov. Phys. Solid State **4**, 759 (1962)]; C. H. Henry and K. Nassau, Phys. Rev. B **1**, 1628 (1970).

[14] P.J. Dean and D.C. Herbert, in *Excitons*, edited by K. Cho (Springer, Berlin, 1979), p. 55.

[15] L. V. Keldysh, Superlatt. Microstruct. **4**, 637 (1988); D. M. Wittaker and R. J. Elliot, Solid State Commun. **68**, 1 (1988).

[16] M. Kumagai and T. Takagahara, Phys. Rev. B **40**, 12 359 (1989).

[17] G. E. W. Bauer and T. Ando, Phys. Rev. B **38**, 6015 (1988).

[18] L. C. Andreani and A. Pasquarello, Phys. Rev. B **42**, 8928 (1990).

[19] D. B. Tran Thoai, R. Zimmermann, M. Grundmann, and D. Bimberg, Phys. Rev. B **42**, 5906 (1990); R. Zimmermann and D. Bimberg, *ibid.* **47**, 15 789 (1993).

[20] R. Atanasov, F. Bassani, A. D'Andrea, and N. Tomassini, Phys. Rev. B **50**, 14 381 (1994).

[21] R. Winkler, Phys. Rev. B **51**, 14 395 (1995). This paper contains also an extensive list of the previous literature.

[22] A. D'Andrea and R. Del Sole, Phys. Rev. B **41**, 1413 (1990).

[23] G. Platero and M. Altarelli, in *Proceedings of the 20th International Conference on the Physics of Semiconductors*, edited by E. M. Anastassakis and J. D. Joannopoulos (World Scientific, Singapore, 1990).

[24] J. Kusano, G. E. W. Bauer, and Y. Aoyagi, J. Appl. Phys. **75**, 289 (1994).

[25] O. Heller, J. Tignon, J. Martinez-Pastor, Ph. Roussignol, G. Bastard, M. Maaref, V. Thierry-Mieg, and R. Planel, Nuovo Cimento D **17**, 1493 (1995).

[26] M. Fritze, I. E. Perakis, A. Getter, W. Knox, K. W. Goossen, J. E. Cunningham, and S. A. Jackson, Phys. Rev. Lett. **76**, 106 (1996).

[27] P. D. Wang, N. N. Ledentsov, C. M. Sotomayor Torres, I. N. Yassievich, A. Pakhomov, A. Yu. Egovov, P. S. Kop'ev, and V. M. Ustinov, Phys. Rev. B **50**, 1604 (1994).

[28] M. V. Belousov, N. N. Ledentsov, M. V. Maximov, P. D. Wang, I. N. Yasievich, N. N. Faleev, I. A. Kozin, V. M. Ustinov, P. S. Kop'ev, and C. M. Sotomayor Torres, Phys. Rev. B **51**, 14 346 (1995).

[29] Z. S. Piao, M. Nakayama, and H. Nishimura, Phys. Rev. B **53**, 1485 (1996).

[30] R. Cingolani, O. Brandt, L. Tapfer, G. Scamarcio, G. C. La Rocca, and K. Ploog, Phys. Rev. B **42**, 3209 (1990); O. Brandt, R. Cingolani, H. Lage, G. Scamarcio, L. Tapfer, and K. Ploog, *ibid.* **42**, 11 396 (1990); O. Brandt, G. C. La Rocca, A. Heberle, A. Ruiz, and K. Ploog, *ibid.* **45**, 3803 (1992); O. Brandt, H. Lage, and K. Ploog, *ibid.* **43**, 14 285 (1991).

[31] R. Schwabe, F. Pietag, M. Faulkner, S. Lassen, V. Gottschalch, R. Franzheld, A. Bitz, and J. L. Staehli, J. Appl. Phys. **77**, 6295 (1995).

[32] R. C. Iotti and L. C. Andreani, Nuovo Cimento D **17**, 1505 (1995).

[33] G. Bastard, J. A. Brum, and R. Ferreira, in *Solid State Physics: Advances in Research and Applications*, edited by D. Turnbull and H. Ehrenreich (Academic, New York, 1991), Vol. 44, p. 229.

[34] M. Altarelli, in *Semiconductor Superlattices and Interfaces*, Proceedings of the International School of Physics ''Enrico Fermi,'' course LVIII, Varenna, 1991, edited by A. Stella and L. Miglio (North-Holland, Amsterdam, 1993), p. 217.

[35] A. Baldereschi and N. O. Lipari, Phys. Rev. B **3**, 439 (1971).

[36] A. Pasquarello, L. C. Andreani, and R. Buczko, Phys. Rev. B **40**, 5602 (1989); S. Fraizzoli, F. Bassani, and R. Buczko, *ibid.* **41**, 5096 (1990).
[37] G. Bastard, Phys. Rev. B **24**, 5693 (1981).
[38] R. C. Iotti and L. C. Andreani, Semicond. Sci. Technol. **10**, 1561 (1995).
[39] U. Rössler, Solid State Commun. **49**, 943 (1984).
[40] *Semiconductors Physics of Group IV Elements and III-V Compounds*, edited by K.-H. Hellwege and O. Madelung, Landolt-Börnstein, New Series, Group III, Vol. 17, Pt. a (Springer, Berlin, 1982).
[41] F. H. Pollak, in *Strained-Layer Superlattices: Physics*, edited by T. P. Pearsall, Semiconductors and Semimetals Vol. 32 (Academic, London, 1990), Vol. 32, p. 17.
[42] P. E. Simmonds, M. J. Birkett, M. S. Skolnick, W. I. E. Tagg, P. Sobkowicz, G. W. Smith, and D. M. Whittaker, Phys. Rev. B **50**, 11 251 (1994).
[43] B. Zhang, S. S. Kano, Y. Shiraki, and R. Ito, J. Phys. Soc. Jpn. **62**, 3031 (1993); Phys. Rev. B **50**, 7499 (1994); B. Zhang, S. S. Kano, R. Ito, and Y. Shiraki, Semicond. Sci. Technol. **10**, 443 (1995).
[44] S. Wilke and D. Henning, Phys. Rev. B **43**, 12 470 (1991); K. A. Mäder and A. Baldereschi, in *Optics of Excitons in Confined Systems*, edited by A. D'Andrea, R. Del Sole, R. Girlanda, and A. Quattropani, IOP Conf. Proc. No. 123 (Institute of Physics and Physical Society, Bristol, 1992), p. 341; M. Di Ventra and K. A. Mäder, Phys. Rev. B **55**, 13 148 (1997).
[45] K. Shiraishi and E. Yamaguchi, Phys. Rev. B **42**, 3064 (1990); J. E. Bernard and A. Zunger, Appl. Phys. Lett. **65**, 165 (1994).
[46] M. Gurioli, J. Martinez-Pastor, M. Colocci, A. Bosacchi, S. Franchi, and L. C. Andreani, Phys. Rev. B **47**, 15 755 (1993).
[47] A. Bitz and R. Schwabe (private communication).